



## CO<sub>2</sub> absorption performance in advanced water-lean diamine solvents

Yanjie Xu <sup>a,b</sup>, Tao Wang <sup>a</sup>, Qi Yang <sup>b</sup>, Hai Yu <sup>c</sup>, Mengxiang Fang <sup>a,\*</sup>, Graeme Puxty <sup>c,\*</sup>

<sup>a</sup> State Key Laboratory of Clean Energy Utilization, Zhejiang University, Hangzhou 310027, PR China

<sup>b</sup> CSIRO Manufacturing, Research Way, Clayton, Victoria 3168, Australia

<sup>c</sup> CSIRO Energy, 10 Murray Dwyer Circuit, Mayfield West, NSW 2304, Australia



### ARTICLE INFO

**Keywords:**  
 CO<sub>2</sub> capture  
 Chemical absorption  
 Water-lean solution  
 Energy penalty  
 Viscosity  
 Cyclic capacity  
 Solubility

### ABSTRACT

In an effort to reduce energy penalties, a range of advanced water-lean solutions blended from one of 8 diamines, an organic solvent diluent and water, were screened. The diamines *N,N*-dimethyl-1,3-propanediamine and *N,N*-dimethyl-1,2-ethanediamine with one primary and one tertiary amino group remain homogenous during CO<sub>2</sub> uptake with the addition of cosolvents (1-methyl-2-pyrrolidinone or sulfolane) and are further investigated for absorption and desorption performance compared with their corresponding aqueous solutions. Water-lean solutions with different water concentrations are tested to explain the impact of water content on the solution performance. Physical properties such as density and viscosity are also measured for a versatile evaluation. The results show that diamine water-lean solutions obtain low viscosity, preferable cyclic capacities and rapid absorption and desorption rates. ENH-5% H<sub>2</sub>O (mass ratio DMEDA: NMP: H<sub>2</sub>O = 3:6.5:0.5) shows the most competitive advantages with comparable viscosity (1.49 mPa•S at 313 K) to aqueous MEA-H<sub>2</sub>O and a 140% improvement in cyclic capacity. Four-fold higher desorption rate is gained ESH-5%H<sub>2</sub>O (mass ratio DMEDA: SFL: H<sub>2</sub>O = 3:6.5:0.5) compared with MEA-H<sub>2</sub>O. Considerable reduction in energy penalties is expected to be achieved in diamine water-lean solutions. In addition, the equilibrium solubility of diamine water-lean solutions also shows potential for industrial application due to their sensitivity to CO<sub>2</sub> partial pressure in contrast with aqueous solutions.

### 1. Introduction

It is expected that coal will still account a large portion of energy resources in 2040, even though the increase in renewable energy and efficiency improvement will slow the need for coal consumption [1]. Moreover, the Intergovernmental Panel on Climate Change (IPCC) proposed a new plan of limiting global warming to 1.5 °C rather than 2 °C above preindustrial levels [2], increasing the need to reduce carbon dioxide emissions from fossil fuels such as coal and gas combustion.

Among the different approaches to capture CO<sub>2</sub>, chemical absorption is the leading technology for Post-combustion carbon capture (PCC) [3–5]. Monoethanolamine (MEA), as a typical commercial solution, has been tested in many industrial applications to demonstrate this viable CO<sub>2</sub> capture technology [6–8]. As an efficient CO<sub>2</sub> capture solution, MEA satisfies the essential needs for fast CO<sub>2</sub> absorption rate and reversible absorption–desorption process. However, the high energy consumption of MEA-based PCC technology hinders its industrial application [9].

To mitigate this limitation, water-lean solutions have attracted the

attention of researchers. This concept involves the use of solutions with a significantly lower water content. Water-lean solutions are designed to reduce energy consumption by replacing water with stable organic cosolvents that have lower specific heat capacities. A low water content can also considerably reduce water vaporization, resulting in a decrease in latent heat in the desorption process. A number of amines [10,11], ionic liquids [12,13] and aminosilicones [14,15] were selected to blend with an organic cosolvent as water-lean solutions. Ionic liquid [16]-based solutions suffer from high viscosity and high cost, as does aminosilicone [17]. The viscosity of GAP-0 in Triethylene glycol (TEG) was ~ 1300 mPa•S at 40 °C, which was approximately 600 times higher than that of 30% MEA under the same conditions [18]. Thus, small molecular structure amine-based water-lean solutions were suggested to overcome the “high viscosity” hump. This type of solution uses glycol derivatives as cosolvents and was first reported by Fluor Corporation in 1939 for combined acid gas removal-dehydration [19]. Sada et al. investigated the reaction kinetics and the mechanism of a nonaqueous (alcoholic) solution of Monoethanolamine (MEA) in 1986 [20]. Song et al. reported that CO<sub>2</sub> solubility in MEA + Ethylene glycol/Polyethylene glycol (EG/

\* Corresponding authors.

E-mail addresses: [mxfang@zju.edu.cn](mailto:mxfang@zju.edu.cn) (M. Fang), [Graeme.Puxty@csiro.au](mailto:Graeme.Puxty@csiro.au) (G. Puxty).

PEG) solutions gradually decreased as EG/PEG mass fractions increased, and this downward change was lower than that of aqueous MEA solution with the same MEA proportion [21]. The glycol derivatives mentioned above were used not only as cosolvents but also as physical absorbents. Nevertheless, CO<sub>2</sub> loading using this kind of cosolvent was low and easily cross-reacted with degradation products [22]. Kortunov et al. investigated other cosolvents, such as sulfolane (SFL) and dimethyl sulfoxide, due to their nonvolatility, good stability and low corrosivity [23]. The sensible and latent heat were substantially decreased by 59% and 12%, respectively, using 2 M Diethylenetriamine (DETA) blended with 3 M SFL [24]. In this blend, the solution was biphasic after CO<sub>2</sub> absorption. SFL was also found to have an unfavorable effect on the CO<sub>2</sub> solubility of mixed solution based on Methyldiethanolamine (MDEA), piperazine (PZ) and SFL [25]. In addition, another cosolvent, 1-methyl-2-pyrrolidinone (NMP), has considerable potential to be applied to water-lean solutions [26,27]. NMP was originally used as a physical solvent for CO<sub>2</sub> absorption at high pressure (>2 MPa) [28]. Due to its advantages, such as excellent thermal stability and good CO<sub>2</sub> physical solubility, a nonaqueous solution blended with 2-amino-2-methyl-1-propanol (AMP) and NMP were investigated by Svensson's group [29]. Unexpectedly, a solid precipitate and relatively low CO<sub>2</sub> capacity were found during the absorption process. Hence, due to its miscibility with both water and organic solutions, a semiaqueous solution containing MEA, water and NMP was evaluated by Rochelle's group [30]. A favorable CO<sub>2</sub> absorption rate was achieved in this solution; however, its high viscosity was considered to cause a reduction in capacity.

Water-lean solution is a good option for CO<sub>2</sub> capture needs but still faces some challenges. It is preferable to improve the performance of water-lean solutions by seeking novel amines with superior performance. Hence, aqueous solutions with diamines containing two amino groups per molecule have also attracted considerable attention. Diamines combine the advantages of different amine functional groups (primary, secondary, tertiary) and can enhance the molecular efficiency. Several groups have investigated the performance of aqueous diamine solutions. Yang et al. first evaluated a number of diamines in CO<sub>2</sub> absorption and desorption [31]. The majority of these amines were shown to have a higher cyclic capacity than PZ. This can help lower the operation cost of a PCC process. Based on the research above, the effects of carbon chain length, amino functional group types and substituents of linear diamines were further investigated. The results showed that 3-diethylaminopropylamine (DEAPA) with a longer carbon chain length (C3) containing ethyl substituents on tertiary amino groups yielded better performance than 3-Dimethylaminopropylamine (DMPDA) and 3-piperidinopropylamine (3PDPA) [32,33]. The highest equilibrium solubility (1.412 mol CO<sub>2</sub>/mol amine) was achieved in 2 M DEAPA solution at 313 K and 101 kPa CO<sub>2</sub>. The work of Yu et al. summarized the kinetic and mass transfer behavior of diamines and provided another method for the selection of novel aqueous diamines [34,35]. Xiao et al. identified a number of cyclic diamines that had comparable CO<sub>2</sub> absorption rates and outstanding cyclic capacities compared with linear diamines [36]. An improvement of 215% was shown for aqueous 4-amino-1-propylpiperidine (4-A1PPD) based on an MEA solution. However, several disadvantages, such as a higher viscosity than MEA, were also identified.

The good solubility of diamines in both water and organic solvents makes them attractive candidates as absorbents in water-lean solutions to remove CO<sub>2</sub>. It is expected that a diamine-based water-lean solution can maintain favorable features such as high molecular efficiency and significantly reduce the energy consumption compared with that of aqueous solutions. Hellebrant et al. mentioned that a nonaqueous solution of diamines containing two secondary amino groups generated solids, while diamines containing one secondary amine and one tertiary amine became very viscous after CO<sub>2</sub> absorption [37]. It was found that the biphasic solution of DMPDA blended with poly(ethylene glycol) dimethylether (NHD) achieved a substantially high CO<sub>2</sub> capacity (1.06 mol CO<sub>2</sub>·mol<sup>-1</sup> amine), resulting in a 42% decrease in energy

consumption compared with MEA aqueous solution [38]. Additionally, designer diamine-based water-lean solutions have not been adequately investigated.

In this work, eight different diamines blended with different mass fractions of SFL and NMP were screened as the first but crucial step in the selection of a suitable homogenous formula for diamine-based water-lean solutions. The diamines evaluated herein all have the most straightforward structures in their own category, which was intended to determine the different impacts of the structural features. Eight homogenous water-lean solutions were selected to further evaluate their absorption and desorption abilities. The effects of carbon chain length and the type of amino groups were also elucidated. Additionally, the physical properties, including the density and viscosity, of different solutions were measured. MEA blends with cosolvents were also investigated as a benchmark for comparison.

## 2. Experimental section

### 2.1. Chemicals

Gaseous carbon dioxide (CO<sub>2</sub>, 99.9%) and nitrogen (N<sub>2</sub>, 99.9%) were supplied by BOC Australia. Abbreviations and molecular structures of the tested amines and cosolvents are displayed in Table S1. Monoethanolamine (MEA, 99% Merck), ethylenediamine (EDA, 99% Aldrich), *N*-methylmethylenediamine (MEDA, 99% Aldrich), *N,N*-dimethyl-1,2-ethanediamine (DMEDA, 99% Sigma), 1,3-diaminopropane (DAP, 99% Alfa Aesar), *N*-methyl-1,3-propanediamine (MAPA, 99% Aldrich), *N,N*-dimethyl-1,3-propanediamine (DMPDA, 99% Aldrich), 1,4-diaminobutane (DAB, 99% Aldrich), 4-amino-1-methylpiperidine (4-A1MPD, 97% Tokyo Chemical Industry Co., LTD), 1-methyl-2-pyrrolidone (NMP, 99% Chem-supply) and sulfolane (SFL, 99% Aldrich) were used as received. The compositions of water-lean solutions investigated in this work are shown in Table 1 with their abbreviations. Deionized water was used to prepare the water-lean solutions.

### 2.2. Experimental section

#### 2.2.1. CO<sub>2</sub> absorption

A schematic diagram of the CO<sub>2</sub> absorption device is displayed in Fig. 1. Amines, organic cosolvent and deionized water were all weighed by an analytical balance, and the weight percentage concentration was used in this paper. Once prepared, the mixed solution was added into a jacketed flask connected with a 40 °C circulating water bath. The stirring rate was 800 rpm during CO<sub>2</sub> absorption controlled by a magnetic stir plate. Inlet gas at an atmospheric pressure containing a 15% volume of CO<sub>2</sub> balanced with N<sub>2</sub> was prepared by a mass flow controller (Bronkhorst High-Tech B.V). The mixed gas was then bubbled into the bottom of the solution with a flow rate of 50 ml/min after presaturation with water. Fourteen samples (0.5 ml) were taken into NMR tubes for analysis at different CO<sub>2</sub> loading points during the 5-hour experiment.

**Table 1**  
Compositions and abbreviations of water-lean solutions studied in this work.

Abbreviation	Amine (wt. %)	Cosolvent (wt. %)	H <sub>2</sub> O (wt. %)
PNH-15% H <sub>2</sub> O	DMPDA (30%)	NMP (55%)	15%
ENH-15% H <sub>2</sub> O	DMEDA (30%)	NMP (55%)	15%
PNH-10% H <sub>2</sub> O	DMPDA (30%)	NMP (60%)	10%
ENH-10% H <sub>2</sub> O	DMEDA (30%)	NMP (60%)	10%
ESH-10% H <sub>2</sub> O	DMEDA (30%)	SFL (60%)	10%
PNH-5% H <sub>2</sub> O	DMPDA (30%)	NMP (65%)	5%
ENH-5% H <sub>2</sub> O	DMEDA (30%)	NMP (65%)	5%
ESH-5% H <sub>2</sub> O	DMEDA (30%)	SFL (65%)	5%
MNH-10% H <sub>2</sub> O	MEA (30%)	NMP (60%)	10%
MEA-H <sub>2</sub> O	MEA (30%)	/	70%
DMPDA-H <sub>2</sub> O	DMPDA (30%)	/	70%
DMEDA-H <sub>2</sub> O	DMEDA (30%)	/	70%

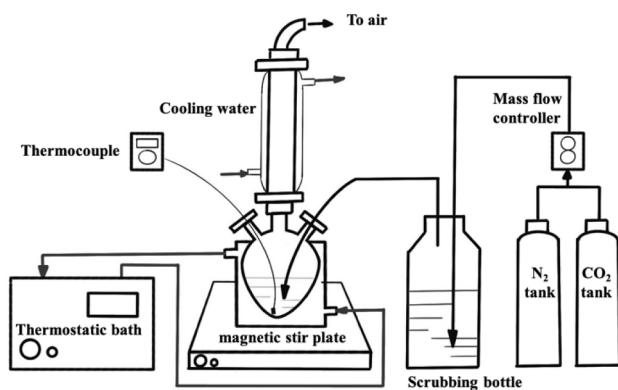


**Fig. 1.** Schematic diagram of CO<sub>2</sub> absorption apparatus.

The remaining loaded solution was reserved for density and viscosity measurements. The equilibrium solubility of the investigated solutions was measured in the same apparatus as used in CO<sub>2</sub> absorption experiments and a method similar to Xiao's study [36]. The CO<sub>2</sub> partial pressure at inlet was changed from 15 to 101 kPa by adjusting the separate flow rates of CO<sub>2</sub> and N<sub>2</sub>. The normalized CO<sub>2</sub> partial pressures related to the impact of water partial pressure on the equilibrium solubility are displayed in the supporting information (Table S2). The first experiment under a 15 kPa CO<sub>2</sub> partial pressure was conducted for 24 h to confirm that initial equilibrium was achieved. The loaded CO<sub>2</sub>-rich solution was used in the next test under a higher CO<sub>2</sub> partial pressure. Thus, the reaction time of the next three tests was reduced to ~10 h to reach subsequent equilibrium after the previous equilibrium step. Four samples with different CO<sub>2</sub> partial pressures were all analyzed by NMR. The accuracy of the experimental methods used in this study was verified previously and the obtained results agreed well with the published data using different methods [33, 39–41]. Moreover, good reproducibility of these experiments was also verified in the laboratory and the results of two examples are displayed in Fig. S1 of supporting information.

#### 2.2.2. CO<sub>2</sub> desorption

The apparatus mentioned above was also used in the CO<sub>2</sub> desorption test. A CO<sub>2</sub>-rich solution (10 ml) obtained from 24 h absorption with a 101 kPa CO<sub>2</sub> pressure (CO<sub>2</sub> flow rate: 25 ml/min) was heated by a circulating water bath at 90 °C and stirred at 800 rpm. Seven samples (0.5 ml) were collected during 60 min of desorption and analyzed by NMR.

#### 2.2.3. Physical property measurement

The density and viscosity of the studied solutions were measured using an Anton Paar DMA 4500 M density meter and an Anton Paar AMVn automated microviscometer at various temperatures. The evaluated temperature ranges of fresh solutions were 20–80 °C. Loaded solutions were only tested at 40 °C. The temperature during the test was maintained within ± 0.1 °C. All samples were analyzed in duplicate to ensure accuracy.

#### 2.2.4. NMR analysis

A Bruker Avance III 400 MHz spectrometer was used for species determination at 20 °C. A sealed capillary containing 13% trioxane in deuterium oxide (D<sub>2</sub>O) was added to the NMR tube as an external standard for signal locking and chemical shift calibration (93.52 ppm) in <sup>13</sup>C NMR spectra. NMR spectra with inverse-gated <sup>1</sup>H decoupling were produced at a pulse angle of 30° (zgjg30 pulse program, Bruker) as the sum of 32 scans with a minimum pulse delay time (D1) of 60 s, which satisfied a value of (AQ + D1) ≥ 5T<sub>1max</sub> of all carbon signals in each sample. TopSpin 3.6 Software was used to process the spectral data.

### 3. Results and discussion

#### 3.1. Solution screening

The homogeneity of the absorbent during the whole process of CO<sub>2</sub> absorption and desorption is a key indicator in selecting an applicable solution for CO<sub>2</sub> capture using the water-lean technique. Therefore, the diamine solutions were first tested for their uniformity up to the maximum CO<sub>2</sub> load with pure CO<sub>2</sub> gas (101 kPa).

The observed results of different water-lean solutions after CO<sub>2</sub> absorption for 24 h are summarized in Table 2. The studied amine in two cosolvents, NMP and SFL, with 10 wt% water were tested initially, and the solutions that were observed for nonhomogenous appearance at any stage during CO<sub>2</sub> absorption were tested with an increased water content (15 wt%). The solution with a water content higher than 15 wt% was not tested because it cannot be exactly defined as a water-lean solution in this case. The amine solution, which remained homogeneous during CO<sub>2</sub> absorption, was tested with a decreased water content (5 wt%) and nonaqueous formulation. In addition, a very small amount of bicarbonate was found by NMR analysis in ENH and PNH with 10 wt% water solutions, and this cannot be simply explained as the impact of water content on the formation of bicarbonate based only on two different water contents (10 wt% and 5 wt%). For this reason, ENH and PNH with 15 wt% H<sub>2</sub>O was tested to better understand this phenomenon. The results in Table 2 show the impact of cosolvent and types of amino groups on the state of the solution. Among the tested amines, only those containing one primary and one tertiary amino group remained homogeneous in the studied water-lean solutions throughout the whole CO<sub>2</sub> absorption process. DMPDA-SFL solution with 10% H<sub>2</sub>O was split into two liquid phases (biphasic) after CO<sub>2</sub> uptake, while the corresponding solution using NMP as the replacement of SFL remained homogeneous. Crystals were formed in solutions containing cyclic diamines, except when mixed 4-A1MPD with 55% SFL and 15% H<sub>2</sub>O, two liquid phases were observed. Furthermore, solutions with two primary amines formed crystals at all the tested water content and cosolvent types during the screening. The viscosity of the solution encompassing amines holding one primary and one secondary amino group, MEDA and MAPA, sharply increased while CO<sub>2</sub> was bubbled into the solution; hence, the solutions were jelly like in their final state. Therefore, solutions containing one tertiary amine are preferably used as water-lean solutions.

#### 3.2. Physical property analysis

We found that physical properties such as density and viscosity play crucial roles in differentiating CO<sub>2</sub> absorption between water-lean and aqueous solutions. Hence, viscosity and density were measured and presented prior to all CO<sub>2</sub> absorption and desorption studies.

##### 3.2.1. Density

The density of the studied fresh solutions was measured in the temperature range of 293 K ~ 353 K, and the results are displayed in Fig. 2 (the numerical results are listed in Table S3). Density of amines and cosolvents obtained by CRC Handbook of Chemical and Physics was also quoted in Table 3 to show the impact of background density.

It is shown in Fig. 2 that all densities decreased with increasing temperature. Among three aqueous solutions, higher density was achieved in MEA-H<sub>2</sub>O [42] compared with other two diamine aqueous solutions (DMEDA-H<sub>2</sub>O and DMPDA-H<sub>2</sub>O). The difference of background density dominated this phenomenon, in which MEA gained higher density than diamines (see in Table 3). Two SFL solutions of DMEDA (ESH) had obviously higher densities than the rest of the solutions due to the higher density of SFL, appearing as parallel curves at the top of Fig. 2. Between them, the ESH solution with a lower water content (5%) had a higher density, which reached 1.0912 g·cm<sup>-3</sup> at 293 K. The MNE-10% H<sub>2</sub>O solution had a higher density than the aqueous MEA solution

**Table 2**  
Water-lean Solution Screening Results.

H <sub>2</sub> O proportion	0%H <sub>2</sub> O		5%H <sub>2</sub> O		10%H <sub>2</sub> O		15%H <sub>2</sub> O	
Cosolvent Abbr.	NMP-70%	NMP-65%	SFL-65%		NMP-60%	SFL-60%	NMP-55%	SFL-55%
MEA-30%				Homogeneous				
EDA-30%				Crystalline	Crystalline	Crystalline	Crystalline	Crystalline
MEDA-30%				Jelly like	Jelly like	Jelly like	Jelly like	Jelly like
DMEDA-30%	Crystalline	Homogeneous	Homogeneous	Homogeneous	Homogeneous	Homogeneous	Homogeneous	Homogeneous
DAP-30%				Crystalline	Crystalline	Crystalline	Crystalline	Crystalline
MAPA-30%				Jelly like	Jelly like	Jelly like	Jelly like	Jelly like
DMPDA-30%	Crystalline	Homogeneous		Homogeneous	Biphasic	Homogenous	Biphasic	Biphasic
DAB-30%				Crystalline	Crystalline	Crystalline	Crystalline	Crystalline
4-A1MPD-30%				Crystalline	Crystalline	Crystalline	Crystalline	Biphasic

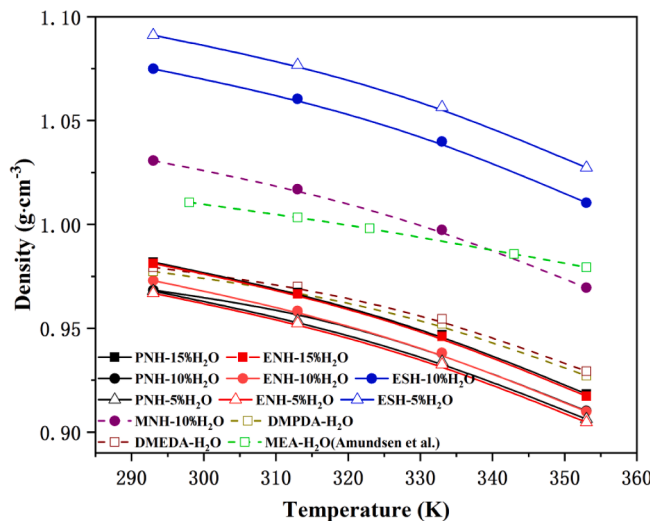


Fig. 2. Density of fresh water-lean solutions versus temperature.

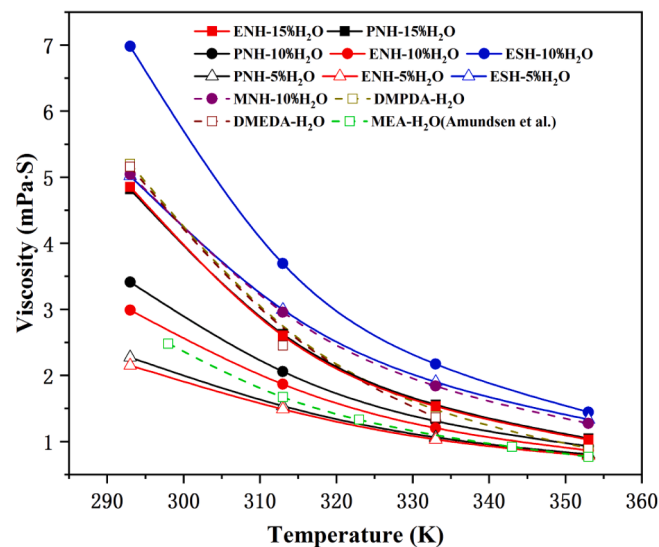


Fig. 3. Viscosity of fresh water-lean solutions as a function of temperature.

**Table 3**  
Density and viscosity of amines and cosolvents mentioned in this work.

Amine	Density* (g·cm <sup>-3</sup> ) at 293 K	Viscosity (mPa·S) at 313 K
MEA	1.0180	9.55
DMEDA	0.8030	0.94
DMPDA	0.8272	1.48
NMP	1.0230	1.49
SFL	1.2723	8.32

\*obtained by <https://hbcp.chemnetbase.com/>.

at a relatively low temperature, but the two curves tended to converge when the temperature increased. The aqueous MEA solution had an even higher viscosity than MNH at 353 K, resulting in their curves intersecting. Regarding diamine-based solutions, the aqueous diamine solutions obtained densities comparable to those of their parallel water-lean solutions with 15% H<sub>2</sub>O. As the temperature increased, the gap between the aqueous and water-lean solutions became wider. This result indicated that the density of the water-lean solutions was more sensitive to temperature variation.

Density values decreased when the water content in the solution was reduced in both ENH and PNH solutions. The parallel water-lean blends of these two diamines displayed similar density curves. Among all the diamine solutions using NMP as a cosolvent, ENH-5% H<sub>2</sub>O had a slightly lower density than other solutions, which is a ~6% reduction compared to that of aqueous MEA.

### 3.2.2. Viscosity

The viscosities of fresh solutions are also measured and shown in Fig. 3, and the numerical results are listed in Table S4. The impact of

background viscosity was also considered. The viscosity of three amines and two cosolvents was tested and exhibited in Table 3.

Fig. 3 shown that all viscosity values decreased as the temperature increased. Similar trends were found with density in the comparison of the aqueous and water-lean solutions based on three amines (MEA, DMEDA and DMPDA). The superiority of the aqueous MEA solution [42] became unapparent with increasing temperature. Diamine (DMEDA and DMPDA) aqueous solutions achieved similar viscosities to their corresponding water-lean solutions containing 15 wt% H<sub>2</sub>O.

The viscosity of fresh water-lean solutions can approximately be ranked as ESH-10% H<sub>2</sub>O > ESH-5% H<sub>2</sub>O ≈ MNH-10% H<sub>2</sub>O > PNH-15% H<sub>2</sub>O > ENH-15% H<sub>2</sub>O > PNH-10% H<sub>2</sub>O > ENH-10% H<sub>2</sub>O > PNH-5% H<sub>2</sub>O > ENH-5% H<sub>2</sub>O.

Among three diamine water-lean solutions, ESH had the highest viscosity due to the higher background viscosity of SFL compared with that of NMP (see in Table 3), but it was more sensitive to the change in temperature, and the gap between the ESH and ENH solutions became narrower as the temperature increased. The ENH solution had a slightly lower viscosity than the PNH solution containing the same water content due to the different background viscosity of DMEDA and DMPDA. Similarly, the MNH-10% H<sub>2</sub>O gained higher viscosity than both ENH and PNH solutions, which was attributed to the higher background viscosity of MEA. Moreover, the hydroxyl group of MEA can enhance the hydrogen bond between the amine and H<sub>2</sub>O molecules, resulting in higher viscosity.

Water content also had a crucial impact on viscosity as it did on density. Similar variations in viscosity with changing water content as observed for density were seen in water-lean solutions. In the measured water content range (5 ~ 15%), the increase in water content was

related to an increase in viscosity, but the impact of water content decreased as the temperature increased.

The viscosity of the studied diamine solutions with different  $\text{CO}_2$  loadings was also measured at 313 K and is presented in Fig. 4. For the sake of comprehensively understanding the viscosity variation between aqueous and water-lean solutions, only one water ratio (10 wt%) of the three water-lean solutions was tested in this case. A similar trend of viscosity was observed in the rich solutions. ESH containing a more viscous cosolvent (SFL) obtained the highest viscosity during the whole  $\text{CO}_2$  absorption process. A viscosity of 8.97 mPa·S under 0.762 mol  $\text{CO}_2 \cdot \text{mol}^{-1}$   $\text{CO}_2$  loading was observed in ENH-10%  $\text{H}_2\text{O}$ , showing the lowest viscosity among the three diamine solutions (ENH, ESH and PNH). The viscosities of all solutions increased with increasing  $\text{CO}_2$  loading. However, the increase in water-lean solution viscosity became more dramatic when  $\text{CO}_2$  loading approached 0.4 mol  $\text{CO}_2 \cdot \text{mol}^{-1}$ . From this point, the gap between the three water-lean systems became much larger. The viscosity of the aqueous system gradually increased until reaching  $\sim 0.4$  mol  $\text{CO}_2 \cdot \text{mol}^{-1}$ , after which it remained unchanged.

It is illustrated that ENH-10%  $\text{H}_2\text{O}$  shown its huge advantage on viscosity even in  $\text{CO}_2$  rich condition, achieving comparable viscosity with published blended solutions like DMEA/PZ (9 mPa·S) [43] and AMP/PZ (5.6 mPa·S) [44] and even four order of magnitude lower viscosity than water lean solution: GAP-0 in TEG ( $\sim 1300$  mPa·S) [17].

### 3.3. $\text{CO}_2$ absorption

#### 3.3.1. Analysis of speciation by $^{13}\text{C}$ NMR spectra

Quantitative  $^{13}\text{C}$  NMR technology is commonly used in speciation studies to identify and quantify different carbon-based species in the reaction system, including amines, carbamate and carbonate/bicarbonate. The signals of carbonate and bicarbonate cannot be separated due to rapid proton exchange, and only one peak is shown in the spectra, which reflects the total proportion of carbonate and bicarbonate. An example of species present in ENH is displayed in Fig. 5.

The stacked  $^{13}\text{C}$  NMR spectra of DMEDA in ENH-15%  $\text{H}_2\text{O}$  solution at different  $\text{CO}_2$  absorption times are presented in Fig. 6. The letters a ~ d and a'~c' are related to different carbon-containing moieties of each species associated with DMEDA, carbamates marked with superscript dots. The peaks of NMP, 51.1 ppm (f), 17.4 ppm (g), 30.7 ppm (h), 174.7 ppm (i) and 31.9 ppm, are not displayed in Fig. 6 to highlight the amine-related signals. As these cosolvents were relatively unfavorable for polar compound formation, only trace amounts of carbonate/bicarbonate formed in the water-lean solutions, which was harder than that in the

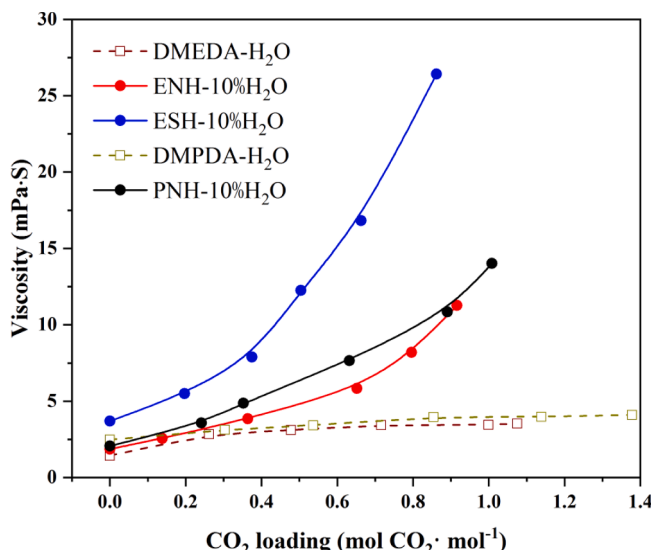


Fig. 4. Viscosity versus  $\text{CO}_2$  loading at 313 K.

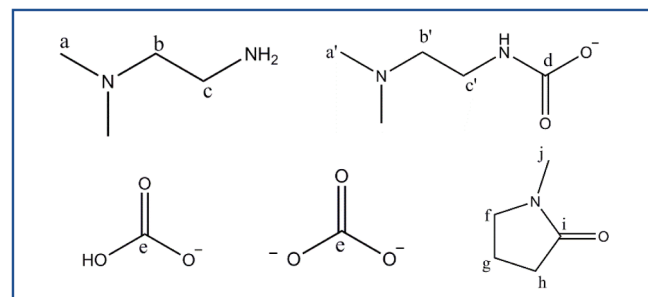


Fig. 5. Species in ENH solutions before and after  $\text{CO}_2$  absorption.

corresponding aqueous system to quantify with high accuracy by NMR. The formed bicarbonate/carbonate concentration can vary in different solutions, which will be discussed in the corresponding sections below. All carbonate/bicarbonate signals observed in the water-lean solutions appeared at a very late stage of  $\text{CO}_2$  absorption, and the pH of the system at this stage should promote the formation of bicarbonate over carbonate. To simplify the discussion, bicarbonate is used below for the sum of carbonate and bicarbonate in all water-lean and aqueous solutions.

#### 3.3.2. $\text{CO}_2$ absorption performance

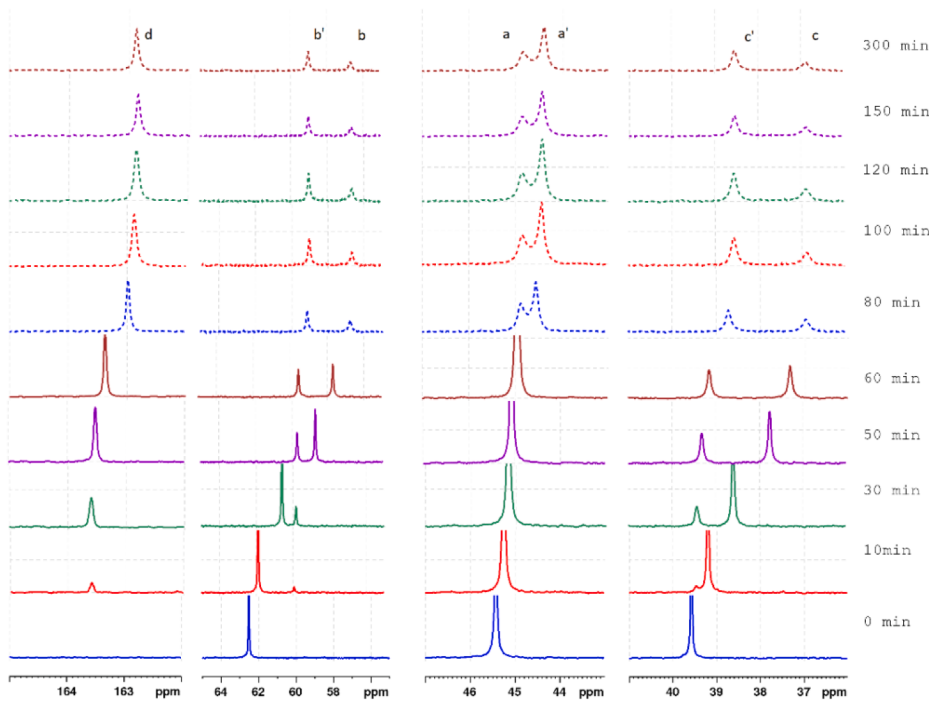
The total molar  $\text{CO}_2$  loading against amines was calculated based on quantitative NMR results. The  $\text{CO}_2$  loading changes of each solution versus absorption time are presented in Fig. 7. The speciation associated with these  $\text{CO}_2$  absorptions is presented in Figs. 8 and 9. The ratios of bicarbonate are listed in Table 4, as the bicarbonate ratios of water-lean solutions were too small to visualize in the same graphic presentation together with other species.

Fig. 7 shows that the  $\text{CO}_2$  capacity of all (diamines and MEA) aqueous solutions was much higher than that of their corresponding water-lean solutions. It is known that the total capacity of an amine solution is strongly affected by bicarbonate formation in the reaction with  $\text{CO}_2$ , as this changes the amine/ $\text{CO}_2$  ratio from 2:1 in carbamate to 1:1 in bicarbonate. The formation of bicarbonate increases the theoretical stoichiometric capacity of amines in the reaction with  $\text{CO}_2$ . Water content plays a key role in bicarbonate formation in two ways: as a hydrolysis reagent and as a polar protic solvent to stabilize bicarbonate ions and their counterions in solution. In contrast, the organic cosolvent in the water-lean solution does not have these functions and thus cannot enhance bicarbonate formation. The water molecules in water-lean systems are significantly diluted by cosolvents; hence, it is harder to perform hydrolysis and solvation as efficiently as in an aqueous system. These factors of bicarbonate formation are the major causes of the lower  $\text{CO}_2$  loading in water-lean solutions. This unfavorability should have a relatively stronger impact on amines that form more bicarbonate in aqueous solutions. This explains why the total  $\text{CO}_2$  capacity change for DMPDA was larger than that for DMEDA in water-lean systems.

The maximum  $\text{CO}_2$  loading of various water-lean solutions was ranked in the order of PNH-15%  $\text{H}_2\text{O}$  (0.786 mol  $\text{CO}_2 \cdot \text{mol}^{-1}$ ) > PNH-10%  $\text{H}_2\text{O}$  (0.775 mol  $\text{CO}_2 \cdot \text{mol}^{-1}$ ) > ENH-5%  $\text{H}_2\text{O}$  (0.767 mol  $\text{CO}_2 \cdot \text{mol}^{-1}$ ) > ENH-10%  $\text{H}_2\text{O}$  (0.762 mol  $\text{CO}_2 \cdot \text{mol}^{-1}$ ) > PNH-5%  $\text{H}_2\text{O}$  (0.743 mol  $\text{CO}_2 \cdot \text{mol}^{-1}$ ) ≈ ENH-15%  $\text{H}_2\text{O}$  (0.741 mol  $\text{CO}_2 \cdot \text{mol}^{-1}$ ) > ESH-10%  $\text{H}_2\text{O}$  (0.729 mol  $\text{CO}_2 \cdot \text{mol}^{-1}$ ) > ESH-5%  $\text{H}_2\text{O}$  (0.681 mol  $\text{CO}_2 \cdot \text{mol}^{-1}$ ) > MNH-10%  $\text{H}_2\text{O}$  (0.589 mol  $\text{CO}_2 \cdot \text{mol}^{-1}$ ).

In PNH and ESH water-lean solutions, a higher water concentration correlated with better maximum loading, while in the ENH water-lean solution, the opposite phenomenon was observed. However, these variations were quite small, and the water-lean solutions of each amine achieved similar total loading within the tested range.

The speciation of different solutions shown in Figs. 8 and 9 can visually elucidate the impact of the water ratio on bicarbonate formation, which also validates the hypothesis discussed above about the



**Fig. 6.** Stacked  $^{13}\text{C}$  NMR amine-based spectra of an ENH-15%  $\text{H}_2\text{O}$  solution absorbing  $\text{CO}_2$  for 0–300 min.

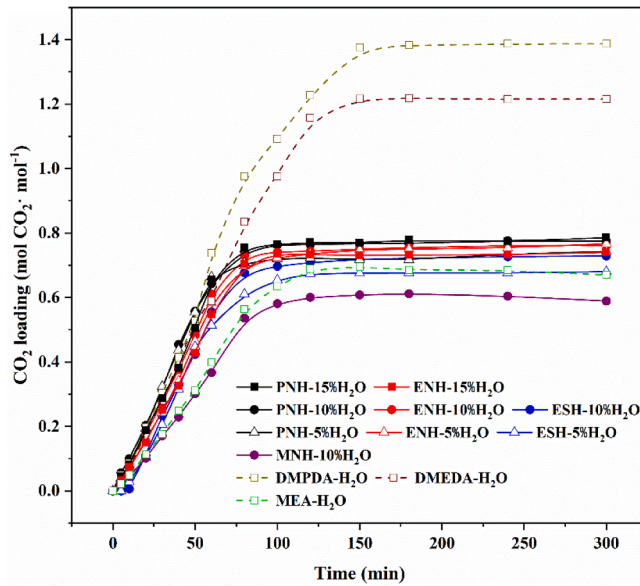


**Fig. 7.**  $\text{CO}_2$  absorption curves of water-lean and aqueous solutions at 40 °C and a  $\text{CO}_2$  partial pressure of 15 kPa.

lower capacity observed in diamine water-lean solutions.

The carbamate ratios of PNH and ENH with the highest water content (15%) are plotted in Fig. 8 together with their corresponding aqueous solutions. MEA and MNH solutions are also displayed for comparison. Bicarbonate was not observed before  $\text{CO}_2$  loading reached 0.6 mol  $\text{CO}_2 \cdot \text{mol}^{-1}$  in the water-lean solutions. Hence, the results of carbamate formation in the water-lean solutions from 0.6 mol  $\text{CO}_2 \cdot \text{mol}^{-1}$  are presented in Fig. 9 to obtain a more detailed view. The blue solid diagonal line in the two figures displays an ideal carbamate ratio trend if carbamate is formed as the sole product in complete  $\text{CO}_2$  absorption. Any formation of bicarbonate will cause the experimental curve to deviate downwards from this line. In the low  $\text{CO}_2$  loading range,

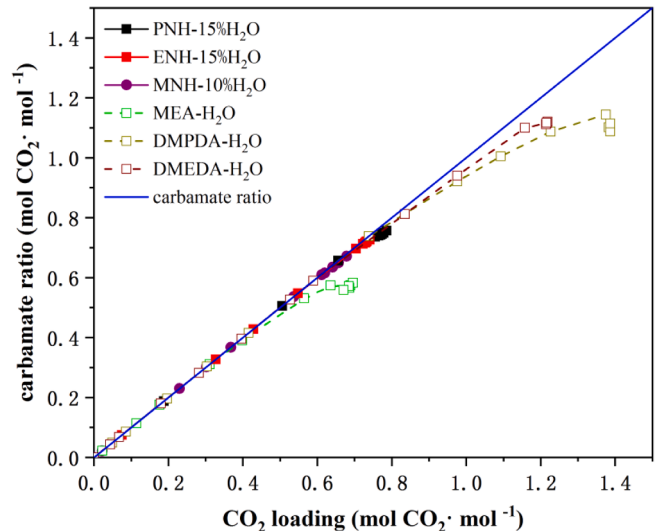


**Fig. 8.** Comparison of carbamate curves between water-lean solutions (15 wt% water content) and aqueous solutions after 5 h of absorption at 40 °C and a  $\text{CO}_2$  partial pressure of 15 kPa.

$\leq 0.6$  in water-lean solutions, all the curves are along the ideal blue line of the carbamate ratio, which reflects that the conversion of carbamates to bicarbonate does not occur at low carbamate concentrations. Fig. 8 shows that the curves of the three aqueous amine solutions deviated more from the blue line than those of all water-lean solutions. This reflects the higher conversion of carbamate to bicarbonate in aqueous solutions. It should be noted that the MEA solutions displayed lower total loading on the basis of mol  $\text{CO}_2 \cdot \text{mol}^{-1}$  amine because it had half the amine functionality of diamines in each molecule.

The bicarbonate ratios of different solutions classified by amines are displayed in Table 4 to achieve a more direct view of the impact of speciation on the total loading. It was observed that the aqueous solutions had the highest bicarbonate formation, and the higher water

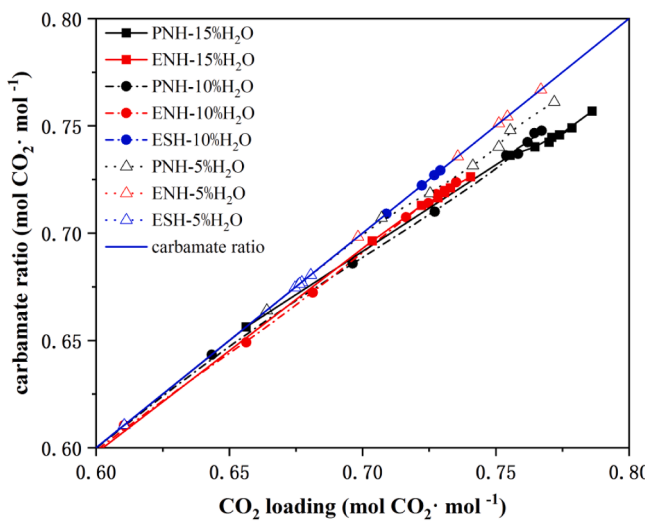


**Fig. 9.** The ratio of carbamate formed in water-lean solutions versus  $\text{CO}_2$  loading.

**Table 4**

Concentration of bicarbonate/carbonate in different water-lean solutions.

Amine	Water content	$C_{\text{bicarbonate}/\text{carbonate}} (\text{mol CO}_2 \cdot \text{mol}^{-1})$
DMPDA	70%	0.273
	15%	0.029
	10%	0.018
	5%	0.011
DMEDA	70%	0.099
	15%	0.014
	10%	0.011
MEA	70%	0.111
	10%	0.007

contents correlated to higher bicarbonate ratios in the corresponding water-lean solutions. Considering amine structures, bicarbonate formation increased from MEA and DMEDA to DMPDA in comparable blends (10% H<sub>2</sub>O). This trend shows the similar structural influence of these amines as in their aqueous systems [36].

### 3.3.3. $\text{CO}_2$ absorption rate

The variation of  $\text{CO}_2$  loading in solutions with time is a good indicator of the  $\text{CO}_2$  absorption rate, although it is not regarded as a strict kinetic measurement [34]. The total  $\text{CO}_2$  loading of each studied solution in the first 30 min is plotted in Fig. 10.

The straight line of each solution is observed in Fig. 10 except for the ESH solution. No carbamate was observed before 10 min in ESH-5% H<sub>2</sub>O and ESH-10% H<sub>2</sub>O solutions during experiments. This was most likely due to the obviously higher viscosity of the ESH-10% H<sub>2</sub>O solution at 40 °C, which slowed  $\text{CO}_2$  diffusion into the solution [45,46]. Although the ESH-5% H<sub>2</sub>O solution had a viscosity value similar to that of MNH-10% H<sub>2</sub>O at 40 °C, its  $\text{CO}_2$  loading at 10 min was lower than that of the MNH-10% H<sub>2</sub>O solution. This indicated that the factor affecting the absorption rate was more than viscosity, e.g., amine reactivity, and its distinct performance with other solutions will be discussed separately. The slopes of the ten straight lines in Fig. 10 reflect the carbamate formation rate and are ranked as PNH-5% H<sub>2</sub>O (10.89E-3) > PNH-10% H<sub>2</sub>O (10.32E-3) > DMPDA-70% H<sub>2</sub>O (10.14E-3) > PNH-15% H<sub>2</sub>O (9.68E-3) > DMEDA-70% H<sub>2</sub>O (9.48E-3) > ENH-10% H<sub>2</sub>O (9.34E-3) > ENH-5% H<sub>2</sub>O (8.36E-3) > ENH-15% H<sub>2</sub>O (8.35E-3) > MEA-H<sub>2</sub>O (6.09E-3) > MNH-10% H<sub>2</sub>O (5.71E-3).

The results show that the absorption rates of different PNH blends are the highest (black lines), those of the ENH series were in the middle (red lines), and those of the MNH solutions were the lowest.  $\text{CO}_2$  was

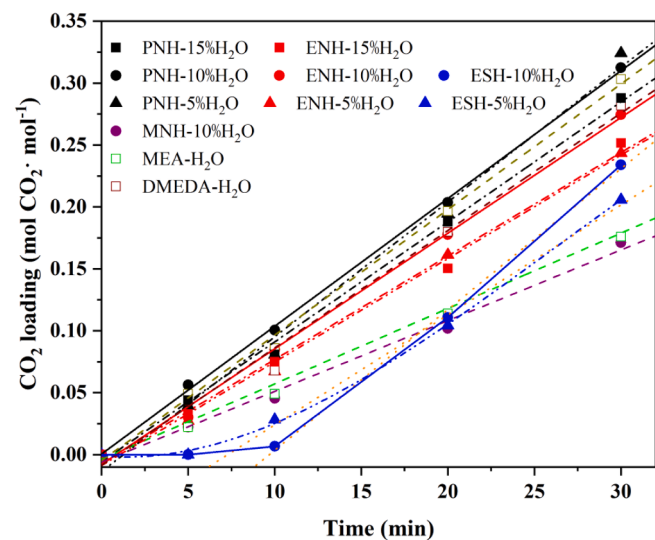


**Fig. 10.**  $\text{CO}_2$  loading versus absorption time in water lean and aqueous solutions: a. dot-and-dashed lines: 15% H<sub>2</sub>O; b. solid lines: 10% H<sub>2</sub>O; c. double dot-and-dashed lines: 5% H<sub>2</sub>O; d. dashed lines: aqueous solutions; e. dotted lines:  $\text{CO}_2$  loading rates of ESH solution from 10 min.

absorbed more rapidly in diamine water-lean solutions than in the aqueous MEA solution. The rate changes versus the amine structural features were similar to the previous study results of aqueous amines [36]. This indicates that amine structures play critical roles in  $\text{CO}_2$  absorption.

Regarding MEA-based solutions, the slope of the aqueous MEA solution was slightly larger than that of the MNH solution because of its lower viscosity. Basically, the diamine DMEDA and DMPDA, which contain two amino groups, have more opportunities to trap  $\text{CO}_2$  than MEA under the same conditions, as the tertiary amino groups of these diamines can act as proton acceptors to free primary amino groups and absorb  $\text{CO}_2$ , while MEA needs another primary amine to trap the proton [36].

Comparable  $\text{CO}_2$  absorption rates were found in the aqueous and water-lean solutions of each diamine. Although the viscosities of diamine solutions with different water contents differed (Fig. 3), this difference decreased at the absorption temperature (40 °C), resulting in similar initial  $\text{CO}_2$  absorption rates.

The ESH solutions displayed totally different curves because their zero-loading period lasted for the initial five minutes. SFL as a cosolvent plays an important role in  $\text{CO}_2$  loading. It has been reported that SFL shows lower  $\text{CO}_2$  solubility than NMP [47]. This feature delayed  $\text{CO}_2$  absorption in the water-lean SFL solutions at the very beginning of the loading time. The orange dotted lines in Fig. 10 show the  $\text{CO}_2$  absorption rate of two ESH solutions with available carbamate data. The slopes of  $\text{CO}_2$  uptake were 11.36E-3 and 8.88E-3 in ESH-10% H<sub>2</sub>O and ESH-5% H<sub>2</sub>O solutions, respectively. The rates of ESH solutions were even higher than those of PNH-10% H<sub>2</sub>O once the absorption reaction began.

### 3.4. $\text{CO}_2$ desorption and cyclic capacity

In addition to the above discussions,  $\text{CO}_2$  cyclic capacity is also one of the critical parameters to evaluate the solution performance in  $\text{CO}_2$  capture and was defined as the molar ratio of  $\text{CO}_2$  released from the desorption process versus amines (Equation (1)).

$$\text{Cyclic capacity} = \frac{\text{mole of } \text{CO}_2 \text{ released}}{\text{mole of amine in the solution}} \quad (1)$$

$\text{CO}_2$  desorption was investigated at 90 °C using  $\text{CO}_2$ -rich aqueous and water-lean solutions containing DMEDA and DMPDA. The results,

together with those of MEA aqueous and water-lean solutions, are plotted in Fig. 11. From these outcomes, the cyclic capacity and desorption rate in the initial 2 min of all studied solutions were calculated and are shown in Fig. 12.

The results in Fig. 11 display more rapid decreases in the desorption curves of all diamine water-lean solutions in the initial time range (2 min) compared to their corresponding aqueous solutions. These results require a different interpretation from that for aqueous solutions, in which bicarbonate decomposition is normally linked with efficient desorption performance. In the water-lean solutions, however, a very small amount of bicarbonate was formed during  $\text{CO}_2$  absorption. The maximum molar  $\text{CO}_2$  loading ratio for all water-lean solutions was <1 even under a  $\text{CO}_2$  pressure of 101 kPa, and their speciation results showed much less bicarbonate formed than that in the aqueous solutions. This phenomenon can be explained by a basic rule: "like seeks like". Nonprotic polar cosolvents, such as NMP and SFL, can stabilize polar carbamate to a certain stage to ensure its formation but have a weaker solvation ability than protic solvents such as water, which have a strong solvation capacity for polar species via hydrogen bonds. The water molecules in water-lean systems are isolated by cosolvent dilution and reduce their solvation ability to polar species via hydrogen bonds. Thus, the weaker solvation and stabilizing effect on carbamates in water-lean systems allow for carbamate decomposition to occur with lower energy consumption. On the other hand, strong solvation and hydrogen bonds readily stabilize carbamate and bicarbonate in an aqueous system; hence, bicarbonate decomposition largely contributes to  $\text{CO}_2$  desorption, while most of the stabilized carbamate remains unchanged. The MEA-based water-lean solution (MNH-10%  $\text{H}_2\text{O}$ ) contained a hydroxyl group in the molecule, which promoted the solvation of water or hydrogen bond formation between species. All these effects added further stability to MEA-formed carbamate and bicarbonate, resulting in a gentler desorption slope.

The cyclic capacities and relative desorption rates of all discussed solutions are displayed in Fig. 12. Cyclic capacities of reported solutions are also shown for comparison. The initial 2 min was chosen as the duration of the desorption rate calculation because the fast desorption process occurring in this range can provide a comparison of the relative desorption rates of different solutions.

For MEA-based solutions, aqueous MEA- $\text{H}_2\text{O}$  shows a slight advantage in cyclic capacity and desorption rate compared to MNH-10%  $\text{H}_2\text{O}$ . Although carbamate decomposed more easily in MNH-10%  $\text{H}_2\text{O}$  than in MEA- $\text{H}_2\text{O}$ , more bicarbonate formed in MEA- $\text{H}_2\text{O}$ , and its

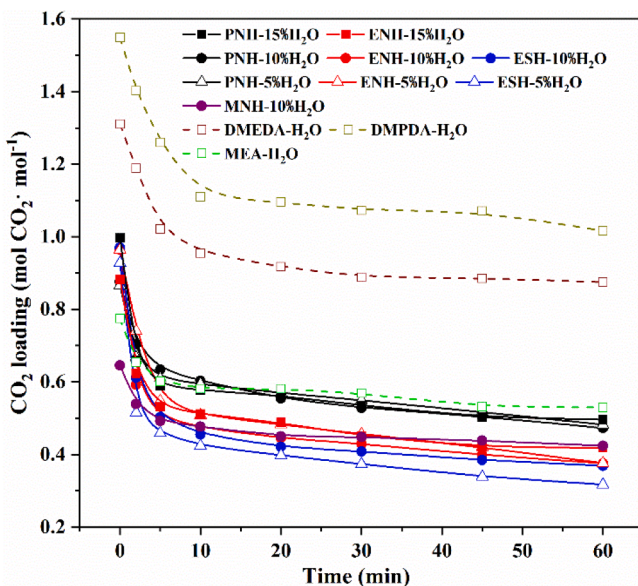


Fig. 11. Desorption curves of water-lean and aqueous solutions at 90 °C.

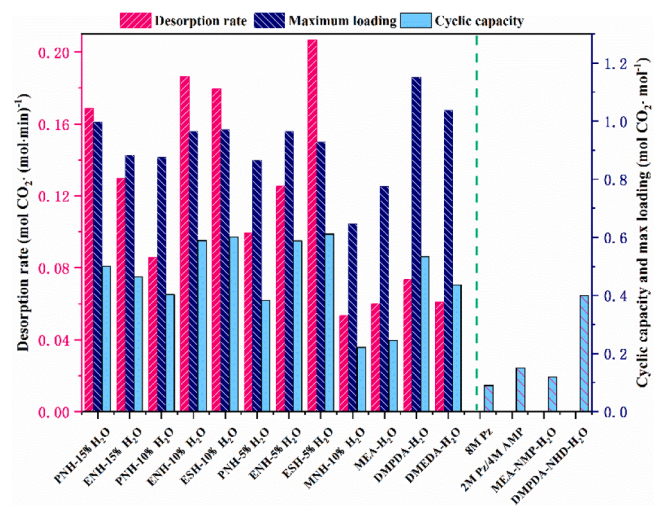


Fig. 12. Comparison of the cyclic capacity (obtained from 60-min desorption test), maximum loading and desorption rate (Desorption rate is calculated as the  $\text{CO}_2$  loading change in the first 2 min divided by the time,  $\text{mol CO}_2 \cdot (\text{mol} \cdot \text{min})^{-1}$ ).

decomposition dominated the desorption process. Hence, similar outcomes of cyclic capacity and desorption rate were achieved in these two MEA-based solutions.

Regarding the studied diamines, all diamine water-lean solutions in this study gain remarkable improvement in their cyclic capacity compared with MEA- $\text{H}_2\text{O}$ , 149% for ESH-5%  $\text{H}_2\text{O}$ , 146% for ESH-10%  $\text{H}_2\text{O}$ , 140% for ENH-10%  $\text{H}_2\text{O}$ , 140% for ENH-5%  $\text{H}_2\text{O}$ , 104% for PNH-15%  $\text{H}_2\text{O}$ , 90% for ENH-15%  $\text{H}_2\text{O}$ , 65% for PNH-10%  $\text{H}_2\text{O}$ , and 57% for PNH-5%  $\text{H}_2\text{O}$ . Compared with other published solutions such as aqueous solution: 8 M PZ [43], blended solution: 2 M PZ/ 4 M AMP [43], water lean solution: MEA-NMP- $\text{H}_2\text{O}$  [30] and biphasic solution: DMPDA-NHD- $\text{H}_2\text{O}$  [38], water lean diamine solutions also shown their obvious superiority on cyclic capacity.

In addition to the desorption rate, a conspicuous advantage is earned in all diamine water lean solutions compared to aqueous MEA, which can be ranked as ESH-5%  $\text{H}_2\text{O}$  > ENH-10%  $\text{H}_2\text{O}$  > ESH-10%  $\text{H}_2\text{O}$  > PNH-15%  $\text{H}_2\text{O}$  > ENH-15%  $\text{H}_2\text{O}$  > ENH-5%  $\text{H}_2\text{O}$  > PNH-5%  $\text{H}_2\text{O}$  > PNH-10%  $\text{H}_2\text{O}$  > DMDPA- $\text{H}_2\text{O}$  > DMEDA- $\text{H}_2\text{O}$  > MEA- $\text{H}_2\text{O}$  > MNH-10%  $\text{H}_2\text{O}$ .

Two solution systems with DMEDA and different cosolvents, ENH and ESH, both exhibited higher cyclic capacities and desorption rates than aqueous DMEDA, which could be attributed to the weaker solvation of NMP and SFL discussed above. A decline in cyclic capacity was observed in the ENH solution by increasing the water content to 15%. It was illustrated that increasing the water content in this case further stabilized the carbamate molecule, retarding its decomposition. Similar cyclic capacities and desorption rates were observed in ENH and ESH solutions with the same water content (10%). Nevertheless, in the comparison of the 5%  $\text{H}_2\text{O}$  solution, an obvious superiority of the desorption rate was seen in ESH-5%  $\text{H}_2\text{O}$ .

In contrast, the cyclic capacity of the DMPDA-based solutions declined gradually with decreasing water content. A 28% reduction in cyclic capacity was obtained in PNH-5%  $\text{H}_2\text{O}$  compared with DMPDA- $\text{H}_2\text{O}$ . It was considered that the composition of bicarbonate dominated the desorption process in this case. More bicarbonate was generated in the solution containing a relatively high water content, which resulted in a higher cyclic capacity. For the desorption rate, the PNH solutions desorbed more rapidly than their corresponding aqueous solution DMPDA- $\text{H}_2\text{O}$ , in which PNH-15%  $\text{H}_2\text{O}$  even reached a 2-times higher desorption rate than DMPDA- $\text{H}_2\text{O}$ .

The tested water-lean solutions of diamines are expected to achieve significant improvement in their energy performance due to their

advantages in cyclic capacity and desorption rate, which is preferable in industrial applications.

### 3.5. Equilibrium solubility

Equilibrium solubility is an important evaluation factor for solutions used in energy simulation, industrial process design and optimization. The CO<sub>2</sub> solubilities of the eight studied water-lean solutions were measured and are displayed in Fig. 13, in which the experimental data of each solution are correlated with trend lines. These results are also presented with aqueous solutions of DMEDA, DMPDA and MEA in Fig. 14 to compare solubility changes in aqueous and water-lean systems as a function of CO<sub>2</sub> partial pressure. As the difference of CO<sub>2</sub> partial pressure before and after normalization (Table S2) was unapparent and not visible in Fig. 14, the inlet CO<sub>2</sub> partial pressure was used below for an easy discussion.

From the results shown in Fig. 13, it was obvious that all PNH solutions had higher CO<sub>2</sub> solubility than the ENH solutions under all CO<sub>2</sub> partial pressures (black lines over red lines), demonstrating the advantage of C3 structural features over C2 features regarding CO<sub>2</sub> solubility. It is also seen that each pair of curves of PNH and ENH solutions with the same ratio of water content displayed a similar type of curve. The curves of 10% water solutions were left of each set of solutions for PNH, ENH and ESH, presenting the lowest CO<sub>2</sub> solubility among each set. As the CO<sub>2</sub> partial pressure increased, these low CO<sub>2</sub> solubilities approached the higher CO<sub>2</sub> loading figures exhibited by other solutions of the same amines with different water contents. This tendency was most obvious under a 101 kPa CO<sub>2</sub> partial pressure, which led to the CO<sub>2</sub> solubility results of all water-lean solution to sit closely at the top of Fig. 13 and produce bent in curves, especially in curves corresponding to a 10% water content. These results suggest that PNH-10% H<sub>2</sub>O is preferable for CO<sub>2</sub> solubility among the tested water-lean solutions.

Unlike water-lean solutions, equilibrium solubility had an explicit linear relation to CO<sub>2</sub> partial pressure in aqueous solutions, and close pressure sensitivity was observed in the three discussed aqueous solutions (MEA-H<sub>2</sub>O, DMEDA-H<sub>2</sub>O and DMPDA-H<sub>2</sub>O). In the current water-lean solution, all the tested diamine solutions were more sensitive than the aqueous MEA solution to variations in CO<sub>2</sub> partial pressure, especially within a relatively high range (Fig. 14). It seemed that the introduction of a cosolvent gave a much higher capacity at higher CO<sub>2</sub> partial pressures. For these reasons, our water-lean solutions are attractive for industrial design and optimization applications.

## 4. Conclusion

In this work, the absorption and desorption performance of advanced water-lean diamine solutions were investigated after preliminary screening of their homogeneity. It was concluded that water-lean diamine solutions obtained low viscosities, which was preferable for cyclic capacities and rapid absorption and desorption rates. A comparable viscosity (1.49 mPa·s at 313 K) to that of aqueous MEA-H<sub>2</sub>O as well as excellent cyclic capacity with 140% improvement were obtained in ENH-5% H<sub>2</sub>O. Moreover, higher desorption rates were achieved in all water lean diamine solutions, in which ESH-5%H<sub>2</sub>O gained approximately four-fold higher desorption rate compared with MEA-H<sub>2</sub>O. Lower energy penalties are expected to be achievable in water-lean diamine solutions due to the lower water content and increased CO<sub>2</sub> desorption during the regeneration process, which is desired in industrial applications. In addition, the equilibrium solubility of water-lean diamine solutions also show potential for industrial application due to their sensitivity to CO<sub>2</sub> partial pressure in contrast with aqueous solutions.

### Declaration of Competing Interest

The authors declare that they have no known competing financial

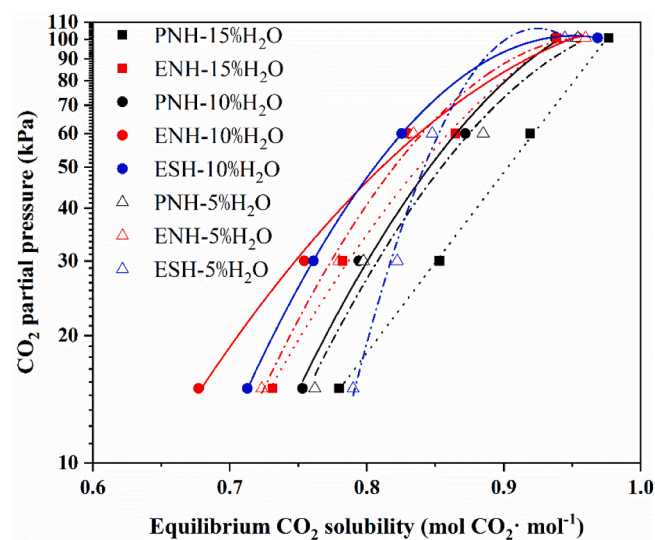


**Fig. 13.** Equilibrium CO<sub>2</sub> solubility of diamine-based water-lean solutions; a: dotted lines: 15 wt% H<sub>2</sub>O; b: solid lines: 10 wt% H<sub>2</sub>O; c: dot-and-dashed lines: 5 wt% H<sub>2</sub>O.

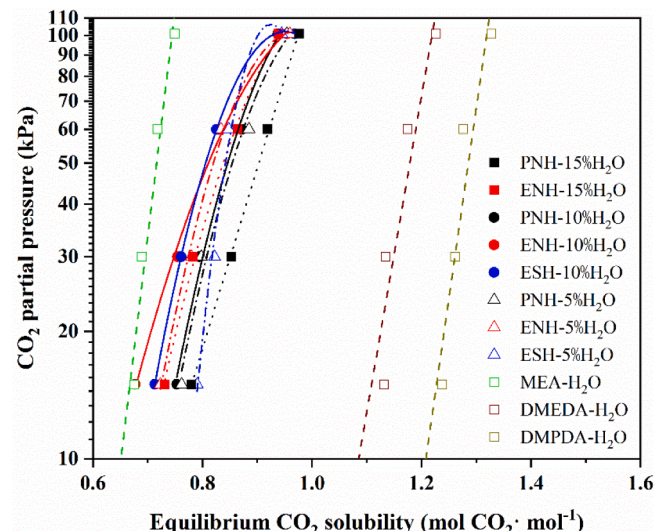


**Fig. 14.** Comparison of equilibrium solubility between water-lean and aqueous diamine solutions- a: dotted lines: 15 wt% H<sub>2</sub>O; b: solid lines: 10 wt% H<sub>2</sub>O; c: dot-and-dashed lines: 5 wt% H<sub>2</sub>O; d: dashed lines: aqueous solutions.

interests or personal relationships that could have appeared to influence the work reported in this paper.

### Acknowledgments

We gratefully acknowledge the financial support from the National Key R&D Program of China (No. 2017YFB0603300). Yanjie Xu is grateful to CSIRO for a visiting student scholarship and the opportunity to work in their laboratories and access their resources.

### Appendix A. Supplementary data

Supplementary data to this article can be found online at <https://doi.org/10.1016/j.cej.2021.131410>.

## References

- [1] International Energy Agency (IEA), World Energy Outlook 2018: The Future is Electrifying, 2018. <https://www.iea.org/workshops/world-energy-outlook-2018-the-future-is-electrifying.html>.
- [2] T. Academy, R. Academy, S.S. Trakt, IPCC\_SR15\_SPM\_version\_report, n.d.
- [3] G. Rochelle, E. Chen, S. Freeman, D. Van Wagener, Q. Xu, A. Voice, Aqueous piperazine as the new standard for CO<sub>2</sub> capture technology, *Chem. Eng. J.* 171 (3) (2011) 725–733, <https://doi.org/10.1016/j.cej.2011.02.011>.
- [4] M. Boscherini, F. Miccio, E. Papa, V. Medri, E. Landi, F. Doghieri, M. Minelli, The relevance of thermal effects during CO<sub>2</sub> adsorption and regeneration in a geopolymers-zeolite composite: Experimental and modelling insights, *Chem. Eng. J.* 408 (2021) 127315, <https://doi.org/10.1016/j.cej.2020.127315>.
- [5] D. Hospital-Benito, J. Lemus, C. Moya, R. Santiago, V.R. Ferro, J. Palomar, Techno-economic feasibility of ionic liquids-based CO<sub>2</sub> chemical capture processes, *Chem. Eng. J.* 407 (2021) 127196, <https://doi.org/10.1016/j.cej.2020.127196>.
- [6] H.C. Mantripragada, H. Zhai, E.S. Rubin, Boundary Dam or Petra Nova – Which is a better model for CCS energy supply? *Int. J. Greenh. Gas Control.* 82 (2019) 59–68, <https://doi.org/10.1016/j.ijggc.2019.01.004>.
- [7] J. Jenkins, Financing mega-scale energy projects: a case study of the petra nova carbon capture project prepared for the ceo council for sustainable urbanization, Paulson Inst. (2015). <http://www.paulsoninstitute.org/wp-content/uploads/2015/10/CS-Petra-Nova-EN.pdf>.
- [8] S. Gao, L. Liu, A. Frank, J. Wang, M. Chris, D. Guo, C. Keith, H. Niu, D. Joanna, X. Wang, S. Wang, B. Roberto, S. XU, China's first pilot-scale demonstration of post-combustion CO<sub>2</sub> capture from a natural-gas-fired power plant, *Greenh. Gases Sci. Technol.* 6 (2) (2016) 178–187, <https://doi.org/10.1002/ghg.2016.6.issue-210.1002/ghg.1557>.
- [9] T. Li, T.C. Keener, A review: Desorption of CO<sub>2</sub>from rich solutions in chemical absorption processes, *Int. J. Greenh. Gas Control.* 51 (2016) 290–304, <https://doi.org/10.1016/j.ijggc.2016.05.030>.
- [10] F. Barzaghi, S. Lai, F. Mani, Novel non-aqueous amine solvents for reversible CO<sub>2</sub> capture, *Energy Procedia* 63 (2014) 1795–1804, <https://doi.org/10.1016/j.egypro.2014.11.186>.
- [11] M.K. Kang, S. Bin Jeon, J.H. Cho, J.S. Kim, K.J. Oh, Characterization and comparison of the CO<sub>2</sub> absorption performance into aqueous, quasi-aqueous and non-aqueous MEA solutions, *Int. J. Greenh. Gas Control.* 63 (2017) 281–288, <https://doi.org/10.1016/j.ijggc.2017.05.020>.
- [12] M.T. Mota-Martinez, P. Brandl, J.P. Hallett, N. Mac Dowell, Challenges and opportunities for the utilisation of ionic liquids as solvents for CO<sub>2</sub> capture, *Mol. Syst. Des. Eng.* 3 (3) (2018) 560–571, <https://doi.org/10.1039/C8ME00009C>.
- [13] Z.-Z. Yang, D.-e. Jiang, X. Zhu, C. Tian, S. Brown, C.-L. Do-Thanh, L.-N. He, S. Dai, Coordination effect-regulated CO<sub>2</sub> capture with an alkali metal onium salts/crown ether system, *Green Chem.* 16 (1) (2014) 253–258, <https://doi.org/10.1039/C3GC41513A>.
- [14] M.J. O'Brien, R.L. Farnum, R.J. Perry, S.E. Genovese, Secondary amine functional disiloxanes as CO<sub>2</sub> sorbents, *Energy Fuels* 28 (5) (2014) 3326–3331, <https://doi.org/10.1021/ef500387t>.
- [15] G.A. Whyatt, A. Zwoster, F. Zheng, R.J. Perry, B.R. Wood, I. Spiriy, C.J. Freeman, D. J. Heldebrandt, Measuring CO<sub>2</sub> and N<sub>2</sub>O Mass Transfer into GAP-1 CO<sub>2</sub>-Capture Solvents at Varied Water Loadings, *Ind. Eng. Chem. Res.* 56 (16) (2017) 4830–4836, <https://doi.org/10.1021/acs.iecr.7b0019310.1021/acs.iecr.7b00193.s001>.
- [16] B. Gurkan, B.F. Goodrich, E.M. Mindrup, L.E. Ficke, M. Massel, S. Seo, T.P. Senftle, H. Wu, M.F. Glaser, J.K. Shah, E.J. Maginn, J.F. Brennecke, W.F. Schneider, Molecular design of high capacity, low viscosity, chemically tunable ionic liquids for CO<sub>2</sub> capture, *J. Phys. Chem. Lett.* 1 (24) (2010) 3494–3499, <https://doi.org/10.1021/jz101533k>.
- [17] R.J. Perry, J.L. Davis, CO<sub>2</sub> capture using solutions of alkanolamines and aminosilicones, *Energy Fuels* 26 (4) (2012) 2512–2517, <https://doi.org/10.1021/ef201963m>.
- [18] R. Perry, T. Grocela-Rocha, M. O'Brien, S. Genovese, B. Wood, L. Lewis, H. Lam, G. Soloveichik, M. Rubinsztajn, S. Krajanski, S. Draper, R. Enick, J.K. Johnson, H.-B. Xie, D. Tapriyal, Aminosilicone solvents for CO<sub>2</sub> capture, *ChemSusChem.* 3 (8) (2010) 919–930, <https://doi.org/10.1002/cssc.201000077>.
- [19] A.J.L. Hutchinson, Process for treating gases (1939).
- [20] E. Sada, H. Kumazawa, Y. Osawa, M. Matsuuwa, Z.Q. Han, Reaction kinetics of carbon dioxide with amines in non-aqueous solvents, *Chem. Eng. J.* 33 (2) (1986) 87–95, [https://doi.org/10.1016/0300-9467\(86\)80038-7](https://doi.org/10.1016/0300-9467(86)80038-7).
- [21] J.-H. Song, S.-B. Park, J.-H. Yoon, H. Lee, K.-H. Lee, Solubility of carbon dioxide in monoethanolamine + ethylene glycol + water and monoethanolamine + poly (ethylene glycol) + water at 333.2 K, *J. Chem. Eng. Data* 42 (1) (1997) 143–144, <https://doi.org/10.1021/je960203w>.
- [22] U. Shoukat, E. Baumeister, D.D.D. Pinto, H.K. Knuutila, Thermal stability and corrosion of tertiary amines in aqueous amine and amine-glycol-water solutions for combined acid gas and water removal, *J. Nat. Gas Sci. Eng.* 62 (2019) 26–37, <https://doi.org/10.1016/j.jngse.2018.11.025>.
- [23] P. Kortunov, L.S. Baugh, D.C. Calabro, M. Siskin, High CO<sub>2</sub> to amine adsorption capacity CO<sub>2</sub> scrubbing processes, (2015).
- [24] L. Wang, S. Yu, Q. Li, Y. Zhang, S. An, S. Zhang, Performance of sulfolane/DETA hybrids for CO<sub>2</sub> absorption: Phase splitting behavior, kinetics and thermodynamics, *Appl. Energy* 228 (2018) 568–576, <https://doi.org/10.1016/j.apenergy.2018.06.077>.
- [25] M. Hosseini Jenab, M. Abedinzadegan Abdi, S.H. Najibi, M. Vahidi, N.S. Matin, Solubility of carbon dioxide in aqueous mixtures of N-methyldiethanolamine + piperazine + sulfolane, *J. Chem. Eng. Data* 50 (2) (2005) 583–586, <https://doi.org/10.1021/je049666p>.
- [26] L.S. Tan, A.M. Shariff, K.K. Lau, M.A. Bustam, Impact of high pressure on high concentration carbon dioxide capture from natural gas by monoethanolamine/N-methyl-2-pyrrolidone solvent in absorption packed column, *Int. J. Greenh. Gas Control* 34 (2015) 25–30, <https://doi.org/10.1016/j.ijggc.2014.12.020>.
- [27] P. Pakzad, M. Mofarahi, A.A. Izadpanah, M. Afkhamipour, C.H. Lee, An experimental and modeling study of CO<sub>2</sub> solubility in a 2-amino-2-methyl-1-propanol (AMP) + N-methyl-2-pyrrolidone (NMP) solution, *Chem. Eng. Sci.* 175 (2018) 365–376, <https://doi.org/10.1016/j.ces.2017.10.015>.
- [28] IEA GHG, Co<sub>2</sub> Capture in the Cement Industry International Energy Agency, (2008). <https://hub.globalecsinstitute.com/sites/default/files/publications/95751/co2-capture-cement-industry.pdf>.
- [29] H. Svensson, J. Edfeldt, V.Z. Velasco, C. Hulteberg, H.T. Karlsson, International Journal of Greenhouse Gas Control Solubility of carbon dioxide in mixtures of 2-amino-2-methyl-1-propanol and organic solvents, *Int. J. Greenh. Gas Control* 27 (2014) 247–254, <https://doi.org/10.1016/j.ijggc.2014.06.004>.
- [30] Y. Yuan, G.T. Rochelle, CO<sub>2</sub> absorption rate in semi-aqueous monoethanolamine, *Chem. Eng. Sci.* 182 (2018) 56–66, <https://doi.org/10.1016/j.ces.2018.02.026>.
- [31] Q. Yang, G. Puxty, S. James, M. Bown, P. Feron, W. Conway, Toward intelligent CO<sub>2</sub> capture solvent design through experimental solvent development and amine synthesis, *Energy Fuels* 30 (9) (2016) 7503–7510, <https://doi.org/10.1021/acs.energyfuels.6b00875.0.1021/acs.energyfuels.6b00875.s001>.
- [32] R. Zhang, Q. Yang, Z. Liang, G. Puxty, R.J. Mulder, J.E. Cosgriff, H. Yu, X. Yang, Y. Xue, Toward efficient CO<sub>2</sub> capture solvent design by analyzing the effect of chain lengths and amino types to the absorption capacity, bicarbonate/carbamate, and cyclic capacity, *Energy Fuels* 31 (10) (2017) 11099–11108, <https://doi.org/10.1021/acs.energyfuels.7b0195110.1021/acs.energyfuels.7b01951.s001>.
- [33] R. Zhang, Q. Yang, B. Yu, H. Yu, Z. Liang, Toward to efficient CO<sub>2</sub> capture solvent design by analyzing the effect of substituent type connected to N-atom, *Energy* 144 (2018) 1064–1072, <https://doi.org/10.1016/J.ENERGY.2017.12.095>.
- [34] B. Yu, H. Yu, K. Li, Q. Yang, R. Zhang, L. Li, Z. Chen, Characterisation and kinetic study of carbon dioxide absorption by an aqueous diamine solution, *Appl. Energy* 208 (2017) 1308–1317, <https://doi.org/10.1016/j.apenergy.2017.09.023>.
- [35] B. Yu, L. Li, H. Yu, M. Maeder, G. Puxty, Q. Yang, P. Feron, W. Conway, Z. Chen, Insights into the chemical mechanism for CO<sub>2</sub>(aq) and H<sup>+</sup> in aqueous diamine solutions - An experimental stopped-flow kinetic and 1H/13C NMR study of aqueous solutions of N, N-Dimethylethylenediamine for Postcombustion CO<sub>2</sub> Capture, *Environ. Sci. Technol.* 52 (2) (2018) 916–926, <https://doi.org/10.1021/acs.est.7b0522610.1021/acs.est.7b05226.s001>.
- [36] M. Xiao, D. Cui, Q. Yang, Z. Liang, G. Puxty, W. Conway, P. Feron, Advanced designer amines for CO<sub>2</sub> capture: Interrogating speciation and physical properties, *Int. J. Greenh. Gas Control.* 82 (2019) 8–18, <https://doi.org/10.1016/j.ijggc.2018.12.021>.
- [37] D.J. Heldebrandt, P.K. Koech, M.T.C. Ang, C. Liang, J.E. Rainbolt, C.R. Yonker, P. G. Jessop, Reversible zwitterionic liquids, the reaction of alkanol guanidines, alkanol amidines, and diamines with CO<sub>2</sub>, *Green Chem.* 12 (2010) 713–721, <https://doi.org/10.1039/b924790d>.
- [38] Y. Qiu, H. Lu, Y. Zhu, Y. Liu, K. Wu, B. Liang, Phase-Change CO<sub>2</sub> absorption using Novel 3-Dimethylaminopropylamine with Primary and Tertiary amino groups, *Ind. Eng. Chem. Res.* 59 (19) (2020) 8902–8910, <https://doi.org/10.1021/acs.iecr.9b06886.0.1021/acs.iecr.9b06886.s001>.
- [39] D. Tong, J.P.M. Trusler, G.C. Maitland, J. Gibbons, P.S. Fennell, Solubility of carbon dioxide in aqueous solution of monoethanolamine or 2-amino-2-methyl-1-propanol: Experimental measurements and modelling, *Int. J. Greenh. Gas Control.* 6 (2012) 37–47, <https://doi.org/10.1016/j.ijggc.2011.11.005>.
- [40] B.K. Choi, S.M. Kim, J.S. Lee, Y.C. Park, D.H. Chun, H.Y. Shin, H.J. Sung, B.M. Min, J.H. Moon, Effect of blending ratio and temperature on CO<sub>2</sub>solubility in blended aqueous solution of monoethanolamine and 2-Amino-2-methyl-propanol: Experimental and Modeling Study Using the Electrolyte Nonrandom Two-Liquid model, *ACS Omega* 5 (44) (2020) 28738–28748, <https://doi.org/10.1021/acsomega.0c04046.0.1021/acsomega.0c04046.s001>.
- [41] P. Singh, Amine based solvent for CO<sub>2</sub> absorption, From molecular structure to process (2011), <https://doi.org/10.3990/1.9789036532006>.
- [42] T.G. Amundsen, L.E. Øi, D.A. Eimer, Density and viscosity of monoethanolamine + water + carbon dioxide from (25 to 80) °C, *J. Chem. Eng. Data* 54 (11) (2009) 3096–3100, <https://doi.org/10.1021/je900188m>.
- [43] L. Li, A.K. Voice, H. Li, O. Namjoshi, T. Nguyen, Y. Du, G.T. Rochelle, Amine blends using concentrated piperazine, *Energy Procedia* (2013) 353–369, <https://doi.org/10.1016/j.egypro.2013.05.121>.
- [44] H. Li, L. Li, T. Nguyen, G.T. Rochelle, J. Chen, Characterization of piperazine/2-aminomethylpropanol for carbon dioxide capture, *Energy Procedia* 37 (2013) 340–352, <https://doi.org/10.1016/j.egypro.2013.05.120>.
- [45] L.M. Galán Sánchez, G.W. Meindersma, A.B. de Haan, Kinetics of absorption of CO<sub>2</sub> in amino-functionalized ionic liquids, *Chem. Eng. J.* 166 (3) (2011) 1104–1115, <https://doi.org/10.1016/j.cej.2010.12.016>.
- [46] L.F. Zubeir, T.M.J. Nijssen, T. Spyriouni, J. Meuldijk, J.R. Hill, M.C. Kroon, Carbon dioxide solubilities and diffusivities in 1-alkyl-3-methylimidazolium tricyanomethane ionic liquids: an experimental and modeling study, *J. Chem. Eng. Data* 61 (12) (2016) 4281–4295, <https://doi.org/10.1021/acs.jcd.6b00657.0.1021/acs.jcd.6b00657.s001>.
- [47] F. Murrieta-Guevara, A. Romero-Martinez, A. Trejo, Gas solubilities of carbon dioxide and hydrogen sulfide in sulfolane and its mixtures with alkanolamines, *Fluid Phase Equilib.* 44 (1988) 105–115, [https://doi.org/10.1016/0378-3812\(88\)80106-7](https://doi.org/10.1016/0378-3812(88)80106-7).